OPEN ACCESS Freely available online

PLOS ONE

Assessing Gibberellins Oxidase Activity by Anion Exchange/Hydrophobic Polymer Monolithic Capillary Liquid Chromatography-Mass Spectrometry

Ming-Luan Chen[1☯], Xin Su[1☯], Wei Xiong[2☯], Jiu-Feng Liu[1], Yan Wu[2], Yu-Qi Feng[1]*, Bi-Feng Yuan[1]*

1 Key Laboratory of Analytical Chemistry for Biology and Medicine (Ministry of Education), Department of Chemistry, Wuhan University, Wuhan, China, **2** College of Life Sciences, Wuhan University, Wuhan, China

Abstract

Bioactive gibberellins (GAs) play a key regulatory role in plant growth and development. In the biosynthesis of GAs, GA3-oxidase catalyzes the final step to produce bioactive GAs. Thus, the evaluation of GA3-oxidase activity is critical for elucidating the regulation mechanism of plant growth controlled by GAs. However, assessing catalytic activity of endogenous GA3-oxidase remains challenging. In the current study, we developed a capillary liquid chromatography – mass spectrometry (cLC-MS) method for the sensitive assay of *in-vitro* recombinant or endogenous GA3-oxidase by analyzing the catalytic substrates and products of GA3-oxidase (GA_1, GA_4, GA_9, GA_{20}). An anion exchange/hydrophobic poly([2-(methacryloyloxy)ethyl]trimethylammonium-*co*-divinylbenzene-*co*-ethylene glycol dimethacrylate)(META-*co*-DVB-*co*-EDMA) monolithic column was successfully prepared for the separation of all target GAs. The limits of detection (LODs, Signal/Noise = 3) of GAs were in the range of 0.62–0.90 fmol. We determined the kinetic parameters (K_m) of recombinant GA3-oxidase in *Escherichia coli* (*E. coli*) cell lysates, which is consistent with previous reports. Furthermore, by using isotope labeled substrates, we successfully evaluated the activity of endogenous GA3-oxidase that converts GA_9 to GA_4 in four types of plant samples, which is, to the best of our knowledge, the first report for the quantification of the activity of endogenous GA3-oxidase in plant. Taken together, the method developed here provides a good solution for the evaluation of endogenous GA3-oxidase activity in plant, which may promote the in-depth study of the growth regulation mechanism governed by GAs in plant physiology.

Citation: Chen M-L, Su X, Xiong W, Liu J-F, Wu Y, et al. (2013) Assessing Gibberellins Oxidase Activity by Anion Exchange/Hydrophobic Polymer Monolithic Capillary Liquid Chromatography-Mass Spectrometry. PLoS ONE 8(7): e69629. doi:10.1371/journal.pone.0069629

Editor: Miyako Kusano, RIKEN PSC, Japan

Received March 26, 2013; **Accepted** June 12, 2013; **Published** July 26, 2013

Funding: The authors thank the financial support from the National Basic Research Program of China (973 Program) (2013CB910702, 2012CB720601), the National Natural Science Foundation of China (91217309, 91017013, 31070327, 21205091, 21228501), Ph.D. Programs Foundation of Ministry of Education of China (20120141120037), the Fundamental Research Funds for the Central Universities, and the Natural Science Foundation of Hubei Province (2011CDB440). The funders had no role in study design, data collection and analysis, decision to publish, or preparation of the manuscript.

Competing Interests: The authors have declared that no competing interests exist.

* E-mail: yqfeng@whu.edu.cn (Y-QF); bfyuan@whu.edu.cn (B-FY)

☯ These authors contributed equally to this work.

Introduction

Gibberellins (GAs), one family of acidic phytohormones, play crucial roles in a number of plant growth and developmental processes, such as seed germination, stem elongation, leaf expansion, and flower development [1,2]. So far, although the number of GAs identified from plants has exceed a hundred, only several GAs, including GA_1, GA_3, GA_4 and GA_7, are considered to function as bioactive plant hormones [3,4]. Previous reports suggest that endogenous developmental cues and environmental signals can affect GAs-controlled plant growth by modulating GAs biosynthesis [5,6]. Therefore, investigation of the regulation of bioactive GAs biosynthesis is crucial for revealing the mechanism of how these hormones control plant developmental processes.

GAs are biosynthesized through an intricate pathway that involves several kinds of enzymes. Recently, the discovery that the GA3-oxidase possesses high catalytic activity in *Arabidopsis thaliana* (*A. thaliana*) embryos during seed germination and development demonstrates that GA3-oxidase plays a key regulatory role in controlling the appropriate levels of bioactive GAs during plant growth [7,8,9,10]. GA3-oxidase is able to catalyze the final step of GAs metabolism to produce the bioactive GAs by converting GA_9 and GA_{20} into bioactive GA_4 and GA_1, respectively (Figure 1) [11]. In some species, GA_9 and GA_{20} are also converted to GA_7 and GA_3, respectively, *via* 2,3-didehydroGA_9 and GA_5, probably as side reactions of GA3-oxidase [12,13]. Although the biosynthetic pathway of GAs catalyzed by GA3-oxidase is established and the genes encoding GA3-oxidase have been isolated from *A. thaliana*, the detection of catalytic activity of endogenous GA3-oxidase remains challenging and no method has been reported for the evaluation of endogenous GA3-oxidase so far.

Mass spectrometry (MS)-based methods have been developed for the analysis of some enzymes activities [14,15,16,17]. The advantage of MS-based enzyme assays has the capacity for simultaneously monitoring the multiple pathways catalyzed by the same enzyme. Gas chromatography-MS (GC-MS) method has been employed for the assessment of *in-vitro* recombinant GA3-oxidase activity expressed from *Escherichia coli* cells [18,19,20]. But the measurement of endogenous activity of GA3-oxidase in plant hasn't been reported, which probably is due to the lack of highly

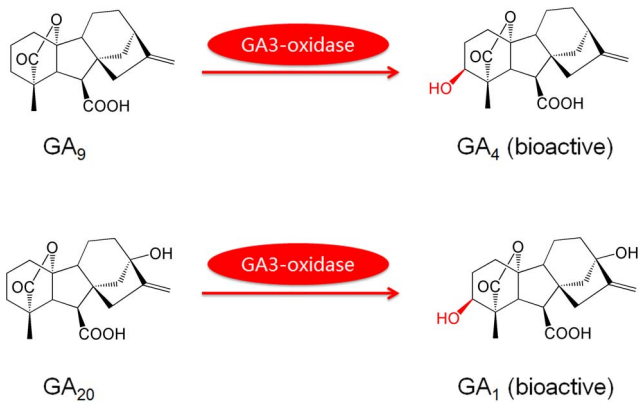

Figure 1. The reactions catalyzed by GA3-oxidase. In each metabolic reaction, the modification is highlighted in red.
doi:10.1371/journal.pone.0069629.g001

sensitive method to analyze the substrates and products of limited endogenous GA3-oxidase. Therefore, researchers normally examined the gene expression levels of the GAs oxidases to estimate the endogenous amount of GAs oxidases [21,22,23,24]. Liquid chromatography-MS (LC-MS) method has been employed to analyze GAs [21,25,26], however, determination of GAs with particulate-packed columns of 2.1 mm internal diameter (*i.d.*) normally requires relatively large amounts of GAs, which may not be sufficient for the analysis of endogenous GA3-oxidase activity in plant samples.

Capillary LC-MS (*c*LC-MS) has been widely used for the ultrasensitive analysis of small molecules [27]. By sensitively analyzing the enzymatic substrates and products, *c*LC-MS may service as a promising method for the accurate assay of endogenous GA3-oxidase activity in small amount plant samples. The porous polymer monolithic columns have several unique properties, such as good pH stability, ease of preparation, and numerous commercial monomers, which can provide good separation resolution towards target analytes with mixed-mode chromatographic retention under isocratic elution condition [28,29,30]. Recently, we prepared a cation exchange/reversed-phase (CX/RP) mixed mode polymer monolithic column and successfully profiled the acidic phytohormones [31], which suggests that evaluation of endogenous GA3-oxidase may be achieved with *c*LC-MS by sensitively analyzing its substrates and products.

Herein, we developed a highly sensitive and simple method for the determination of endogenous GA3-oxidase activity using a poly([2-(methacryloyloxy)ethyl]trimethylammonium-*co*-divinylbenzene-*co*-ethylene glycol dimethacrylate)(META-*co*-DVB-*co*-EDMA) monolithic column coupled with mass spectrometry. With the existence of quaternary ammonium and phenyl groups on the monolithic surface, five GAs (GA_1, GA_4, GA_9, GA_{20} and GA_{53}) were baseline separated by anion exchange/reversed-phase (AX/RP) mixed-mode retention. The in-source collision activated dissociation (CAD) of GAs was suppressed in ESI source by optimizing the ESI conditions. Additionally, a large injection volume (1200 nL) was employed to improve the detection sensitivity. Under optimized conditions, LODs for target GAs range from 0.62 to 0.90 fmol, which is, to the best of our knowledge, the lowest LODs of GAs ever reported without derivatization. Kinetic parameters (K_m) of the recombinant GA3-oxidase were determined to be 1.7 μM and 14.0 μM for GA_9 and GA_{20}, respectively. The developed method was further applied in the evaluation of endogenous GA3-oxidase activity in different types of plant tissues, including rice embryos, rice seedlings, *A. thaliana* seedlings, and *A. thaliana* flowers based on the quantification of isotope labeled catalytic products ($[^2H_2]GA_1$ and $[^2H_2]GA_4$) of GA3-oxidase. The results show that endogenous GA3-oxidase activity can be distinctly determined in all the four types of plant tissues examined.

Materials and Methods

Chemicals

META (80 wt % in H_2O, containing 600 ppm monomethyl ether hydroquinone as the inhibitor), DVB (80 wt %, 1000 ppm *p*-tert-butylcatechol as the inhibitor), and EDMA (98 wt % pure, containing 90–110 ppm MEHQ as inhibitor) were purchased from Acros (New Jersey, USA). To remove inhibitors, DVB and EDMA were extracted with 10% aqueous sodium hydroxide and water; after drying with $MgSO_4$, they were filtered and distilled under reduced pressure. META was directly used without further purification. Azobisisobutyronitrile (AIBN) and PEG-6000 were purchased from Shanghai Chemical Reagent Corporation (Shanghai, China). AIBN was purified by recrystallization from ethanol at 40°C. 3-(Triethoxysilyl) propyl methacrylate was purchased from Wuhan University Silicone New Material (Wuhan, China). HPLC-grade methanol and acetonitrile (ACN) were obtained from TEDIA (Ohio, USA). The water used throughout all experiments was purified using a Milli-Q water purification system (Millipore, Bradford, USA). The fused-silica capillaries with were purchased from Yongnian Optic Fiber Plant (Hebei, China).

Stable isotope-labeled compounds and standards, $[^2H_2]GA_1$, $[^2H_2]GA_4$, $[^2H_2]GA_9$, $[^2H_2]GA_{20}$, $[^2H_2]GA_{53}$, GA_1, GA_4, GA_9, and GA_{20} were all purchased from Olchemim Ltd. (Olomouc, Czech Republic). Thiourea, acrylamide, formic acid (FA), *N*,*N*-dimethylformamide (DMF), ammonium formate ($HCOONH_4$), DL-Dithiothreitol (DTT), phenylmethanesulfonyl fluoride (PMSF), tris(hydroxymethyl)aminomethane, NaCl, NaF, Na_3VO_4, and other chemicals of analytical grade used in the experiment were purchased from Shanghai Chemical (Shanghai, China). The standard solution (100 μg/mL) for each analyte was prepared in methanol and stored at −4°C in the dark.

Preparation and Characterization of Poly(META-*co*-DVB-*co*-EDMA) Monolith

The poly(META-*co*-DVB-*co*-EDMA) monolith was prepared by one-step thermally initiated *in-situ* polymerization. Firstly, porogen PEG-6000 was dissolved in DMF and thoroughly mixed to ensure that the solution was completely homogeneous. Subsequently, META, DVB and EDMA were added in the polymerization mixture. The mixture was then briefly shaken before adding the initiator AIBN (1 wt % of monomers). The polymerization mixture was completely mixed by vortex and ultrasonication to form a homogeneous solution after adding AIBN. Then the resulting solution was filled into the capillary. Both ends of the capillary were sealed by silicon rubber for polymerization at 60°C for 12 h. Finally, the prepared monolithic column was washed with ACN to remove residual reagents, and conditioned by the mobile phase (ACN/H_2O/FA, 60/40/0.6, v/v/v) at 1 μL/min for 1 h.

Poly(META-*co*-DVB-*co*-EDMA) monoliths were also synthesized in Eppendorf vial for the specific surface area measurement. After polymerization, the monolith was cut into small cubic pieces and submersed in ACN/FA (90/10, v/v) for at least 2 h at 60°C to remove the PEG-6000 and non-reacted chemicals. The washing step was repeated three times followed by drying in oven at 80°C.

And the resulting monolithic cubic pieces were kept in a desiccator before characterization.

The specific surface area and mesopore size distribution of the prepared poly(META-*co*-DVB-*co*-EDMA) monoliths were measured by nitrogen adsorption-desorption experiments using a JW-BK specific surface area and pore size analyzer (JWGB Sci & Tech Co., Ltd., Beijing, China). Before measurement, the monolithic cubic pieces were evacuated in vacuum and heated to 120°C for 3 h to remove the physically adsorbed substances. Specific surface area values were determined by the Brunauer-Emmett-Teller (BET) equation at P/P_0 between 0.05 and 0.35 [32]. Mesopore size distributions were determined from the desorption branches of isotherms based on the Barrett-Joyner-Halenda (BJH) model [33].

The microscopic morphology of the monolith was examined by scanning electron microscopy (SEM) using a Quanta 200 scanning electron microscope (FEI Company, Holland). Permeability measurements were performed using a Shimadzu LC-10AT pump (Kyoto, Japan) under the constant flow mode. ACN was pumped through the prepared monolithic column (30 cm-long, 100 μm *i.d.*, 360 μm *o.d.*) at flow rate of 2 μL/min. The back pressure was recorded when the pressure stabilized. Permeability (*K*) was calculated according to Darcy's Law [34].

Expression of GA3-oxidase in *E. coli* Cells

The coding sequences of *Arabidopsis GA3ox1* were cloned into vector pGEX containing Glutathione S-transferase (GST) tag. The *E. coli* cell lysate expressing GST-GA3ox1 was produced according to previously described protocol [8].

Preparation of Plant Samples for Evaluation of Endogenous GA3-oxidase Activity

The plant samples (rice and *A. thaliana*) were grown in a growth chamber in a 16 h light/8 h dark photoperiod with 80% humidity under 28°C. Light intensity was fixed to 120 lux/m^2/s.

All plant samples were collected, weighted, immediately frozen in liquid nitrogen, and then stored at −80°C. Plant samples (2–250 mg) were frozen in liquid nitrogen and finely ground followed by extraction with 8 mL/g cell lysis buffer (25 mM Tris-HCl, pH 7.5, 150 mM NaCl, 2 mM DTT, 1 mM NaF, 0.5 mM Na_3VO_4, 15 mM *β*-glycerophosphate, 0.5 mM PMSF) for 30 min, then centrifuged at 10,000 g under 4°C for 5 min to collect the cell lysates. The cell lysates were concentrated to 100 μL at 4°C using ultrafiltration membrane (30 kDa cutoff; Millipore) for the analysis of endogenous GA3-oxidase activity.

Assessing GA3-oxidase Activity with *c*LC-MS

For enzyme assay, the *E. coli* cell lysates or plant cell lysates (50 μL) were incubated with the substrates (GA_9 and GA_{20} for *E. coli* cell lysates, [$^2H_2$]GA_9 and [$^2H_2$]GA_{20} for plant cell lysates) and the internal standard ([$^2H_2$]GA_{53}) in the presence of 100 mM Tris-HCl (pH 7.5) and cofactor mixture (4 mM 2-oxoglutarate, 5 mM *L*-ascorbate and 5 mM $FeSO_4$) in a total volume of 100 μL. The *E. coli* cell lysate without GA3-oxidase expression was used as negative control. The incubation was performed at 30°C for 3 h and then 150 μL of acetic acid was added to stop the reaction. The resulting solution was lyophilized to dryness and then redissolved in 510 μL H_2O/ACN (10/500, v/v). The mixture was vortexed and centrifuged at 12,000 g under 4°C for 5 min. The supernatant was collected and evaporated under mild nitrogen stream at 25°C followed by reconstituting in 100 μL H_2O/ACN (90/10, v/v) for *c*LC-MS analysis.

Determination of the substrates and products of GA3-oxidase was performed on a Shimadzu Prominence nano-flow liquid chromatography system (Kyoto, Japan) coupled with a Bruker Daltonics micrOTOFq orthogonal-accelerated time-of-flight mass spectrometer (Bremen, Germany). The Shimadzu *c*LC system contains two LC-20AD nano pumps, two vacuum degassers, a LC-20AB HPLC pump, a SIL-20AC HT auto-sampler and a FCV nano valve. The Bruker mass spectrometer is controlled by Bruker Daltonics Control 3.4. Bruker Daltonics Data analysis 3.4 software was employed for the data analysis. Transfer parameters were optimized by direct infusion of an ESI tuning mix from Agilent Technologies (Waldbronn, Germany). Spectra were collected with a time resolution of 50 Hz in the m/z range of 50–600.

The analytical column of poly(META-*co*-DVB-*co*-EDMA) monolithic column (100 μm *i.d.*, 360 μm *o.d.*, 30-cm long) was connected to nano-flow liquid chromatographyand conditioned with the mobile phase at a flow rate of 800 nL/min for 30 min. The poly(META-*co*-DVB-*co*-EDMA) monolithic column was coupled with a ESI emitter (7 cm×25 μm, with a 8±1 μm tip) (PicoTip company, USA) by a stainless steel union. The fused-silica capillaries (50 μm *i.d.*) with different lengths were employed as the 800~1400 nL sample loop (e.g. the volume of 60-cm long capillary was 1200 nL).

Results and Discussion

Preparation of poly(META-*co*-DVB-*co*-EDMA) monolithic column

Using binary crosslinkers, DVB and EDMA, a CX/RP polymer monolith with a large specific surface area was successfully prepared in our previous work [35]. DVB can enhance the crosslinking degree of monolith [36,37], and EDMA can promote to form a homogeneous polymerization mixture when adding hydrophilic/charged functional monomers. Thus, a monolithic column with large specific surface area can be obtained with facile preparation process. In current study, the GA3-oxidase catalytic substrates and products are organic molecules with carboxyl groups; therefore, the positively charged functional monomer META and hydrophobic crosslinkers DVB and EDMA are empolyed to provide a anion-exchnage/RP (AX/RP) mixed-mode chromatographic retention towards analytes.

To obtain the favourable porous structure of the poly(META-*co*-DVB-*co*-EDMA) monolith, the polymerization mixture was optimized (Table S1, S2, S3, Figure S1). The optimized polymerization mixture consists of 3.7% (w/w_{total}) META, 11.0% (w/w_{total}) DVB, 11.0% (w/w_{total}) EDMA, 11.4% (w/w_{total}) PEG-6000, 62.9% (w/w_{total}) DMF and 1% ($w/w_{total\ monomers}$) AIBN.

Characterization of poly(META-*co*-DVB-*co*-EDMA) Monolithic Column

The morphology of the prepared poly(META-*co*-DVB-*co*-EDMA) monolithic column was examined by SEM (Figure 2A–C). Figure 2A shows the coarse surface of microglobules, which indicates the existence of mesopores on the monolithic surface. In addition, the continuous monolithic matrix was obtained and attached well to the inner wall of the monolithic column (Figure 2B) with through-pores of approximate 1.5 μm (Figure 2C). The distribution of mesopore in the poly(META-*co*-DVB-*co*-EDMA) monolith ranges from 3.3 to 4.0 nm, and the specific surface area is 426 m^2/g (Figure 2D), which is comparable to the hypercrosslinked monolithic column [38,39,40].

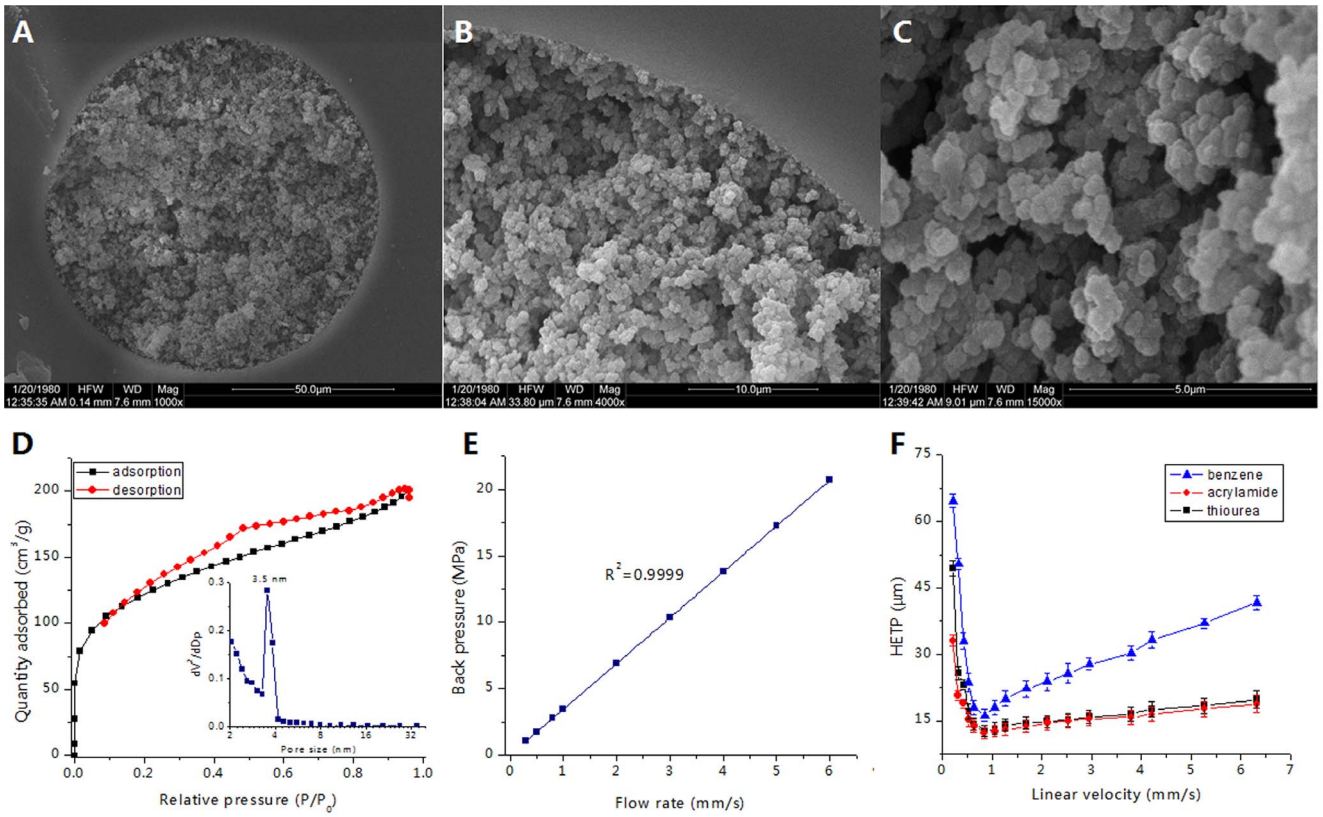

Figure 2. Characterizations of the META-silica hybrid monolithic column. (A) – (C) SEM images. (A) ×1,000 wide-view, (B) ×4,000 close-up-view, and (C) ×15,000 close-up-view. (D) The N_2 isothermal plot with the inset showing the pore-size distribution. (E) The effect of flow rate on the back pressure of the monolithic column. (F) Van Deemter plot of the height equivalent to a theoretical plate as a function of flow rate. Experimental conditions: column, poly(META-*co*-DVB-*co*-EDMA) monolithic column (30-cm long, 100 μm *i.d.*, 360 μm *o.d.*); UV detection wavelength, 254 nm for acrylamide, 214 nm for thiourea and benzene; mobile phase used in (E), ACN; mobile phase used in (F), ACN/H_2O (60/40, v/v).
doi:10.1371/journal.pone.0069629.g002

The mechanical stability of the prepared monolithic column was examined with an increase of flow rate from 100 to 1800 nL/min (linear velocity: 0.21–5.88 mm/s). The results show that the back pressure linearly increases with the increase of the flow rate (Figure 2E), which demonstrates that the monolithic column bed is stable even under high back pressure (~20 MPa).

The column efficiency of the poly(META-*co*-DVB-*co*-EDMA) monolith was evaluated by changing the flow rate from 0.05 to 2.50 mm/s. The effect of the flow velocity on the plate height was examined by using benzene, acrylamide, and thiourea (Figure 2F). The results show the lowest plate height is approximate 12.2 μm for acrylamide with a flow velocity of 0.84 mm/s (~82,000 plates/m). Moreover, under high velocity, the theoretical plate heights of these analytes did not significantly increase, which suggests fast separation of GAs can be implemented with this monolithic column.

The reproducibility of the prepared poly(META-*co*-DVB-*co*-EDMA) monoliths was evaluated by analysis of GA_1, benzene and acrylamide. The run-to-run (n = 10), column-to-column (n = 5) and batch-to-batch (n = 5) variations (RSDs) of these monoliths were 0.9%, 5.7%, and 11.4%, respectively, for retention time of these analytes, and 1.4%, 8.8%, and 13.7%, respectively, for the column efficiency of these three analytes. Additionally, the retention time and column efficiency of analytes and the back pressure of monolithic column did not significantly change even after three-month continuous use. These results indicate that excellent reproducibility of the monoliths can be achieved.

Separation of Target GAs on Poly(META-*co*-DVB-*co*-EDMA) Monolithic Column

We investigated the separation mechanisms and optimized the separation conditions for five GAs (GA_1, GA_4, GA_9, GA_{20}, and GA_{53}) with *c*LC-MS. Since the existent of salt in the mobile phase can lower the MS sensitivity of GAs, buffer solution was not used in the mobile phase for the subsequent experiment.

Firstly, the influence of mobile phase acidity on the retention of GAs was investigated. Without a buffer solution, the addition of formic acid (FA) will lead to the immediate decrease of the mobile phase pH to approximately 3.5, and further increase of FA content could affect the mobile phase pH slightly. Whereas, the ion strength of the mobile phase will increase by adding FA. Thus, we optimized the FA content in the mobile phase instead of the mobile phase pH. In Figure 3A, when the FA content increased from 0.2 to 1% (v/v), the retention factors (k) of GAs decrease. We reason that with the increase of FA content, the degree of ionization of GAs is suppressed and the ion strength of mobile phase increased, therefore, the electrostatic interaction between GAs and the quaternary ammonium groups is weaken, which exhibits typical anion-exchange retention mechanism towards GAs. The increase of ACN content in mobile phase from 10 to 80% (v/v) results in the linear decrease of the retention of GAs (Figure 3B), which indicates the RP retention of the monolithic column. Taken together, the results demonstrate the SAX/RP retention mechanism of poly(META-*co*-DVB-*co*-EDMA) monolithic column towards negatively charged GAs. Considering the

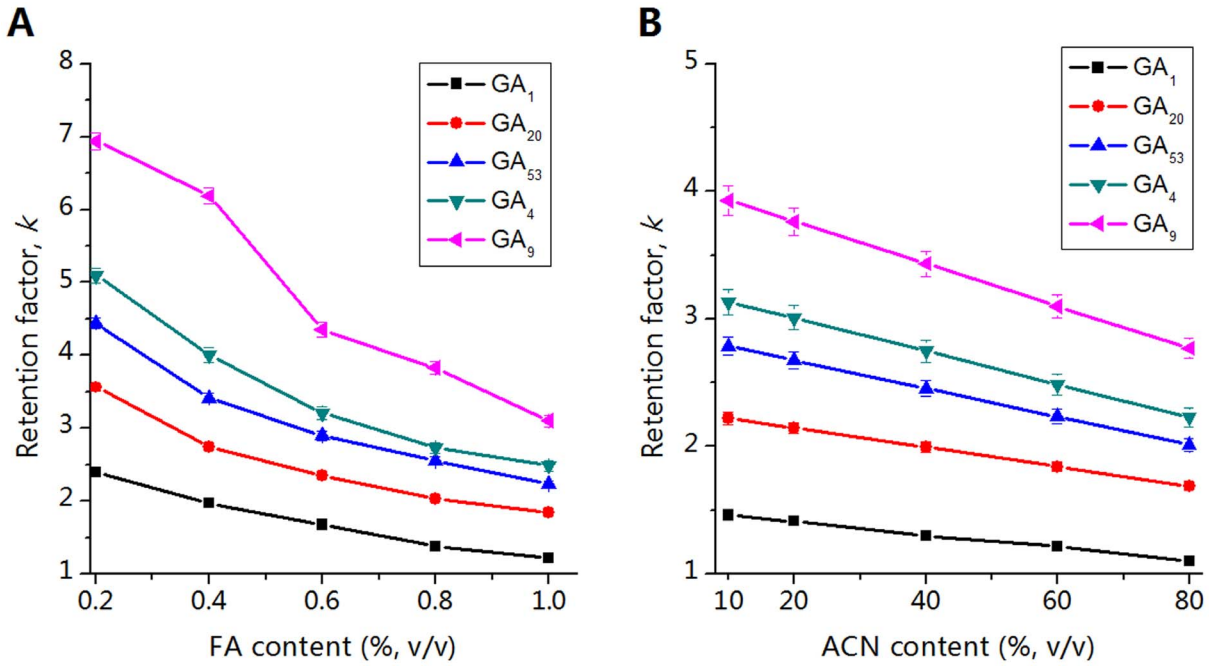

Figure 3. Investigation of the separation mechanisms for five GAs. (A) The effects of FA content on the retention factor (*k*) of GAs. (B) The effects of ACN content on the retention factor (*k*) of GAs. Experimental conditions: column, poly(META-*co*-DVB-*co*-EDMA) monolithic column (30-cm long, 100 μm *i.d.*, 360 μm *o.d.*).
doi:10.1371/journal.pone.0069629.g003

high ACN content can improve the MS response of GAs, ACN content was kept at 60% (v/v) for the subsequent experiment.

In addition, the separation resolution of these analytes was not apparently influenced with a high flow rate (Figure S2). At the flow rate of 500 nL/min, the column efficiencies of 5 GAs are around 75,000 plates/m. With the increase of flow rate, the column efficiencies of all five GAs slightly decreased from 75,000 to 60,000 plates/m, which indicated that this polymer monolithic column with large specific surface area is suitable for the fast separation of acidic small molecules. Yet, the nano-valves and tubes were frequently blocked after sample injection when the back pressure exceeding 10 MPa. Thus, we chose 800 nL/min as the optimal flow rate for the further methodological investigation. Finally, a 14-min baseline separation of 5 GAs was achieved with this poly(META-*co*-DVB-*co*-EDMA) monolithic column using the isocratic elution condition of ACN/H_2O/FA (60/40/0.6, v/v/v) at the flow rate of 800 nL/min (Figure 4).

Optimization of ESI-MS Conditions for Detection of GAs

In previous reports, the acidic phytohormones were frequently analyzed in multiple reaction monitoring (MRM) mode. Whereas, the fragmentation behaviour of GAs hasn't been rigorously investigated. According to the full-scan spectrum (ESI-MS spectrum) of GA_1 (Figure 5A), the $[M - H]^-$ adduct of GA_1 appeared at m/z 347.1494. Also present, however, was the in-source CAD fragment ion at m/z 145.2263, 223.1134, and 241.2413. The intensity of fragment ions at m/z 145.2263 (I_{145}), 223.1134 (I_{223}), and 241.2413 (I_{241}) versus the intensity of GA_1 at m/z 347.1494 (I_{347}) was 1.2/1, 0.9/1, and 1/1, respectively. These observations indicate that GAs was a set of fragile molecules and the in-source CAD occurrence can cause the loss in the detection sensitivity of GAs.

To circumvent this problem, we optimized the in-source ESI-MS conditions to suppress the in-source CAD occurrence of GAs, including funnel radio frequency (RF), collision RF, hexapole RF, capillary voltage, flow rate and temperature of dry gas. The results show that, under optimized in-source ESI-MS conditions (see details in Supporting Information), the I_{145}, I_{223}, and I_{241} versus I_{345} are all lower than 1/10, which increases the detection sensitivity of GA_3 for more than one order of magnitude (Figure 5B). Consequently, the ion of I_{347} (347.1496) was used for the quantification of GA_1. The ESI source conditions for the analysis of other 4 GAs were also optimized using the same strategy (Figure S3).

Methodological Establishment

Since the prepared poly(META-*co*-DVB-*co*-EDMA) monolithic column possesses large specific surface area of 426 m^2/g and fast mass transfer kinetics, a large sample injection volume can be implemented on this monolithic column with no decreased separation resolution. The target GAs can be trapped in the front of analytical monolithic column with aqueous sample matrix. Subsequently, the mobile phase with high ACN can elute GAs from the sample zone. The signal/noise (S/N) ratio for most of the GAs increases with the increase of injection volume from 800 nL to 1200 nL, while the injection volume of 1400 nL results in a decrease of S/N ratio (Table S4), which indicates the diffusion of sample zone on the monolithic column. Consequently, sample injection volume was fixed at 1200 nL for further experiments.

The LODs and LOQs of GAs are calculated as the amounts of the analyte at an S/N ratio of 3 and 10, respectively. The results show the LOD and LOQ were 0.62 and 2.00 fmol for GA_1, and 0.90 and 3.04 fmol for GA_4, respectively (Table 1), which was comparable to that obtained by derivatization method [31,41]. The detection linearity of the method was investigated using the internal standard of 30.0 fmol $[^2H_2]GA_{53}$ spiked with GA_1 and GA_4 at different amounts ranging from 2.00 fmol to 400 fmol. The calibration curve was constructed by plotting the mean peak

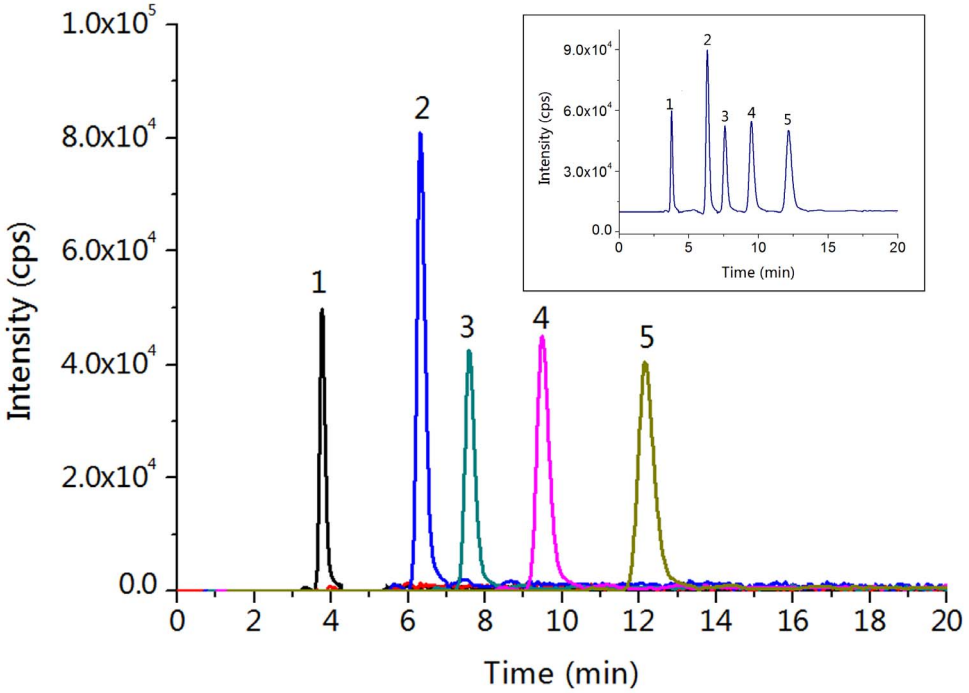

Figure 4. Extracted ion chromatogram of five GA standards. Shown in inset is the total ion chromatogram of five GA standards. Experimental conditions: column, poly(META-*co*-DVB-*co*-EDMA) monolithic column (30-cm long, 100 μm *i.d.*, 360 μm *o.d.*); flow rate, 800 nL/min; mobile phase, ACN/H_2O/FA (60/40/0.6, v/v/v). Order of peaks: 1. GA_1, 2. GA_{20}, 3. GA_{53}, 4. GA_4, 5. GA_9.
doi:10.1371/journal.pone.0069629.g004

area ratio of GA_1 and GA_4 to $[^2H_2]GA_{53}$ versus their molar amount based on data obtained from triplicate measurements. The results show that good linearity within the range of 2.00–400 fmol GAs was obtained with coefficient correlation (R) higher than 0.9971 (Table 1).

We then examined the stabilities of the GA3-oxidase catalytic products ($[^2H_2]GA_1$ and $[^2H_2]GA_4$) and internal standard ($[^2H_2]GA_{53}$) under the enzyme catalytic reaction conditions. The results show that there were no apparent changes of the MS intensities for these analytes in the reaction mixture even for 24 h, which demonstrates that the method is appropriate for the evaluation of endogenous GA3-oxidase activity by measuring GA3-oxidase catalytic products of $[^2H_2]GA_1$ and $[^2H_2]GA_4$.

The effect of matrix on the quantification of these bioactive GAs was evaluated by spiking standards (2.00–400 fmol GA_1, GA_4, and 30 fmol $[^2H_2]GA_{53}$) into *E. coli* cell lysates or isotope standards (2.00–400 fmol $[^2H_2]GA_1$, $[^2H_2]GA_4$, and 30 fmol $[^2H_2]GA_{53}$) into rice seedling matrix. The results show that these GAs can be

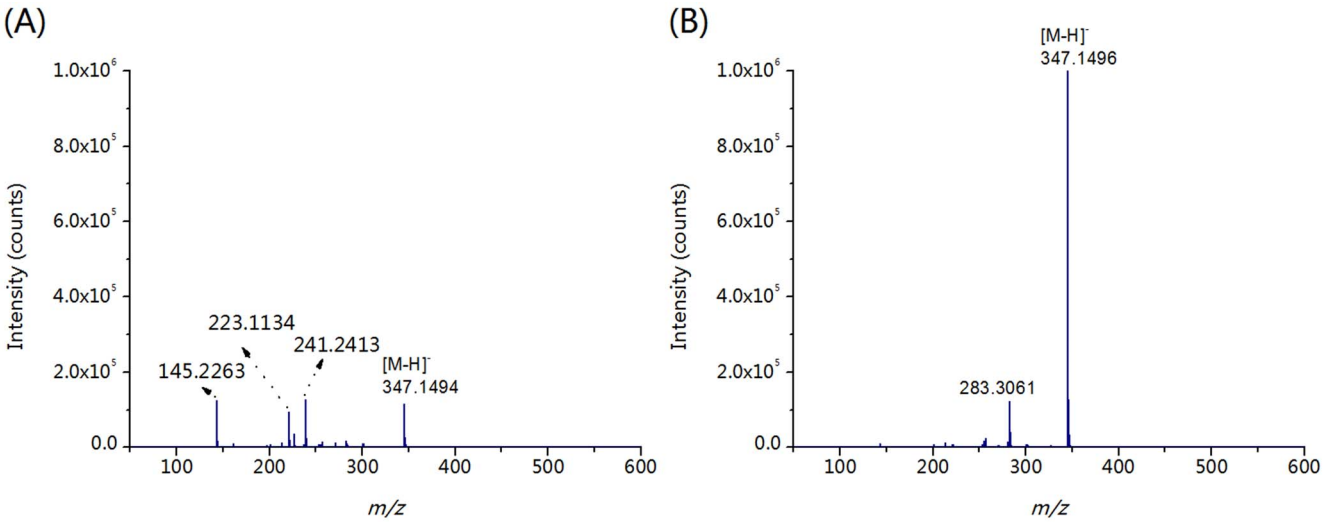

Figure 5. Optimization of the mass spectrometry detection conditions of GA_1. (A) Full-scan spectrum of GA_1. (B) Full-scan spectrum of GA_1 with optimized ESI source conditions. Experimental conditions: 1 μg/mL GA_1 were infused in mobile phase (ACN/H_2O/FA, 60/40/0.6, v/v/v) at a flow rate of 3 μL/min.
doi:10.1371/journal.pone.0069629.g005

Table 1. Linearity, LODs and LOQs of GAs obtained by *c*LC-MS method.

Analytes	Linear range (fmol)	Regression line		R	LOD (fmol)	LOQ (fmol)
		Slope	Intercept			
GA_1	2.00–400	0.0025	−0.0733	0.9971	0.62	2.00
GA_4	2.00–400	0.0041	−0.0961	0.9975	0.90	3.04

doi:10.1371/journal.pone.0069629.t001

successfully determined with 89.5–116.0% recoveries (RSDs, 1.8–11.9%, N = 4) in *E. coli* cell lysates (Table S5) and 80.2–93.2% recoveries in rice seedling matrix (RSDs, 0.2–7.8%, N = 4) (Table S6). Additionally, good intra- and inter-day precision can be achieved, which were manifested by RSDs (N = 5) being less than 11.2% and 13.5% with *E. coli* cell lysates (Table S7) and less than 9.3% and 10.7% with rice seedling matrix (Table S8). Taken together, these results indicate that the *c*LC-MS method is reliable for the quantification of GA3-oxidase catalytic products.

Measurement of GA3-oxidase Activity by *c*LC-MS

The kinetic parameters (K_m) of *in-vitro* recombinant GA3-oxidase determined by our developed *c*LC-MS method was 1.7 μM and 14.0 μM for GA_9 and GA_{20}, respectively (Figure 6), which are consistent with previous reports (1.0–1.5 μM for GA_9, and 13.0–15.0 μM for GA_{20}) [13,14,15,16]. Additionally, the much lower K_m value of GA3-oxidase for GA_9 than GA_{20} suggests the higher catalytic activity of GA3-oxidase towards GA_9 than GA_{20}.

According to previous reports, the endogenous bioactive GAs could be produced by GA3-oxidase catalysis in plant germinating, seedling and flowering [7,8,9,10,42]. However, up to date, the quantification of endogenous GA3-oxidase activity in plant species has not been established. With our developed *c*LC-MS method, we determined the catalytic activity of endogenous GA3-oxidase for converting GA_9 to GA_4 in rice embryos (1.01±0.24 pmol/g/h, n = 3), rice seedlings (0.21±0.03 pmol/g/h, n = 3), *A. thaliana* seedlings (1.77±0.36 pmol/g/h, n = 3), and *A. thaliana* flowers (0.22±0.04 pmol/g/h, n = 3). The extracted ion chromatogram of enzyme catalytic products $[^2H_2]GA_4$ in rice embryos exhibited that the products can be clearly identified and quantified with no interfere (Figure 7). $[^2H_2]GA_1$, which was another GA3-oxidase catalytic product by converting $[^2H_2]GA_{20}$, was not observed even using 1 g plant sample. This result suggests that endogenous GA3-oxidase has much lower catalytic activity towards GA_{20} than GA_9, which is consistent with the results obtained using *in-vitro* recombinant GA3-oxidase (the K_m of recombinant GA3-oxidase for GA_{20} was approximate one order of magnitude larger than that for GA_9).

In addition, we investigated the minimal plant sample required for the quantification of endogenous GA3-oxidase activity. With the decrease of sample amount from 250 to 5 mg, the endogenous GA3-oxidase catalytic activity (pmol/h) linearly decreased (Figure S4). The activity of endogenous GA3-oxidase can be distinctly measured from 5 mg plant samples. Compared to the normal LC-MS method, our developed *c*LC-MS method can achieve much

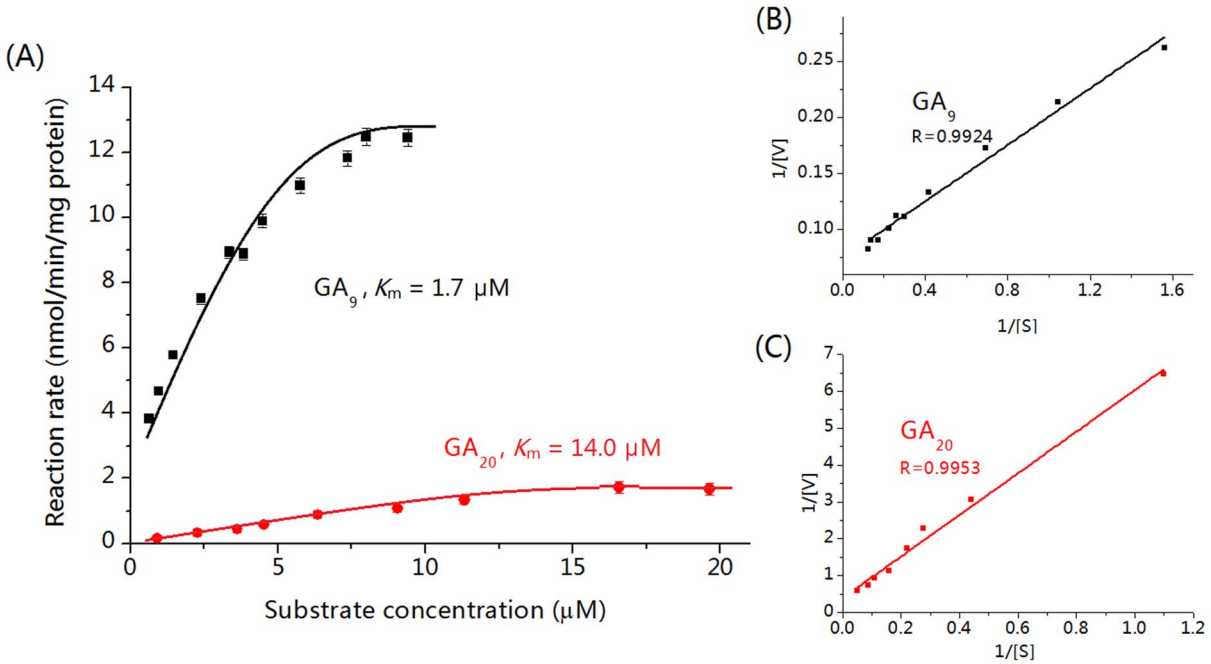

Figure 6. The kinetics study of GA3-oxidase. (A) Michaelis–Menten plots of recombinant GA3-oxidase in *E. coli*. cell lysate. (B) Lineweaver–Burk plots for GA_9. (C) Lineweaver–Burk plots for GA_{20}. Experimental conditions: GA_9 or GA_{20} was incubated for 15 min at 30°C with *E. coli*. cell lysate and cofactors.
doi:10.1371/journal.pone.0069629.g006

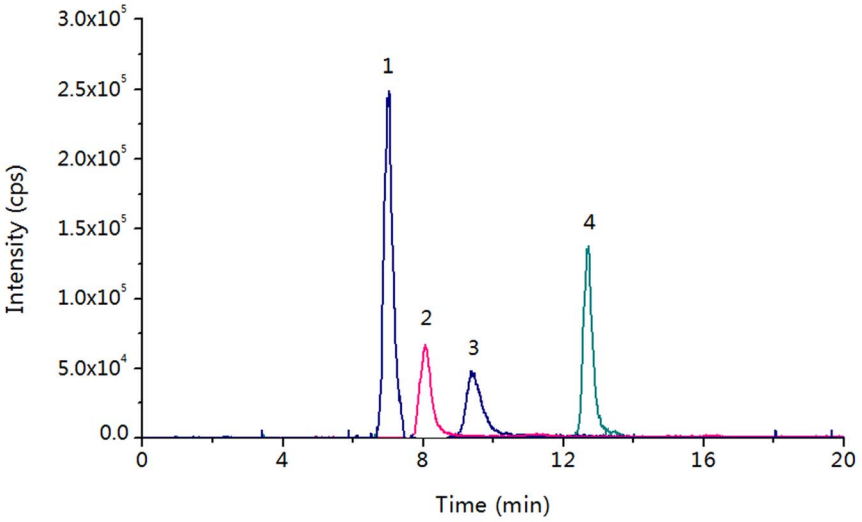

Figure 7. Extracted ion chromatogram of the catalytic products and substrates of GA3-oxidase using 5 mg of rice embryos. Experimental conditions: column, poly(META-*co*-DVB-*co*-EDMA) monolithic column (30-cm long, 100 μm *i.d.*, 360 μm *o.d.*); flow rate, 800 nL/min; mobile phase, ACN/H_2O/FA (60/40/0.6, v/v/v). Order of peaks: 1. [$^2H_2$]GA_{20}, 2. [$^2H_2$]GA_{53} (I.S.), 3. [$^2H_2$]GA_4, 4. [$^2H_2$]GA_9.
doi:10.1371/journal.pone.0069629.g007

better detection sensitivity towards GAs [43], therefore, the low activity of endogenous GA3-oxidase can be easily assessed from small amount plant sample by analyzing its substrates and products.

Conclusions

In this study, we developed a sensitive and robust method for the evaluation of recombinant or endogenous GA3-oxidase activity using poly(META-*co*-DVB-*co*-EDMA) monolithic column coupled with mass spectrometry. With AX/RP mixed-mode chromatographic retention mechanism, the catalytic substrates and products of GA3-oxidase (GA_1, GA_4, GA_9, GA_{20}) and internal standard of [$^2H_2$]GA_{53} were well separated. Using this method, we investigated the K_m of recombinant GA3-oxidase, which was consistent with previous reports. Additionally, the activity of endogenous GA3-oxidase catalyzing the conversion of [$^2H_2$]GA_9 into [$^2H_2$]GA_4 was successfully determined in four different types of plant samples. These results demonstrate the endogenous GA3-oxidase activity can be distinctly measured by our developed *c*LC-MS method, which provides appropriate analytical tool for the further study of the growth regulation mechanism controlled by GAs.

Supporting Information

Text S1 Optimization for the Preparation of Poly(META-*co*-DVB-*co*-EDMA) Monolithic Column.
(DOC)

Text S2 Optimization of ESI-MS Conditions for Detection of GAs.
(DOC)

Table S1 Permeability (*K*) and microscopic images of the monoliths prepared with different amount of PEG-6000.
(DOC)

Table S2 Optimization of the amount of META for the preparation of monoliths.
(DOC)

Table S3 Optimization of the weight of DVB to EDMA for the preparation of monoliths.
(DOC)

Table S4 The signal/noise (S/N) ratios of 4 target GAs with different sample injection volume.
(DOC)

Table S5 Recoveries for the determination of GA3-oxidase catalytic products (GA_1, and GA_4) in *E. coli* cell lysate.
(DOC)

Table S6 Recoveries for the determination of GA3-oxidase catalytic products ([$^2H_2$]GA_1 and [$^2H_2$]GA_4) in rice seedling sample.
(DOC)

Table S7 Precisions (intra- and inter-day) for the determination of GA3-oxidase catalytic products (GA_1 and GA_4) in the matrix of *E. coli* cell lysate.
(DOC)

Table S8 Precisions (intra- and inter-day) for the determination of GA3-oxidase catalytic products ([$^2H_2$]GA_1 and [$^2H_2$]GA_4) in rice seedling sample.
(DOC)

Figure S1 The Scanning electron microscope images of the cross section of monoliths (×16,000 close-up-view).
(DOC)

Figure S2 Extracted ion chromatograms of 5 GAs with different linear velocity.
(DOC)

Figure S3 Full-scan spectra of GAs under optimized ESI source conditions.
(DOC)

Figure S4 The linearity of endogenous GA3-oxidase activity (pmol/h) with different plant weight (mg).
(DOC)

Author Contributions

Conceived and designed the experiments: MLC XS WX YW YQF BFY. Performed the experiments: MLC XS WX JFL. Analyzed the data: MLC XS YW YQF BFY. Contributed reagents/materials/analysis tools: YW YQF BFY. Wrote the paper: MLC XS YW YQF BFY.

References

1. Richards DE, King KE, Ait-ali T, Harberd NP (2001) How gibberellin regulates plant growth and development: a molecular genetic analysis of gibberellin signaling. Annu Rev Plant Physiol Plant Molec Biol 52: 67–88.
2. Olszewski N, Sun TP, Gubler F (2002) Gibberellin signaling: biosynthesis, catabolism, and response pathways. Plant Cell 14 Suppl: S61–80.
3. Yamaguchi S (2008) Gibberellin metabolism and its regulation. Annu Rev Plant Biol 59: 225–251.
4. Achard P, Genschik P (2009) Releasing the brakes of plant growth: how GAs shutdown DELLA proteins. J Exp Bot 60: 1085–1092.
5. Rademacher W (2000) Growth retardants: effects on gibberellin biosynthesis and other metabolic pathways. Annu Rev Plant Physiol Plant Molec Biol 51: 501–531.
6. Kim SG, Lee AK, Yoon HK, Park CM (2008) A membrane-bound NAC transcription factor NTL8 regulates gibberellic acid-mediated salt signaling in Arabidopsis seed germination. Plant J 55: 77–88.
7. Pimenta Lange MJ, Knop N, Lange T (2012) Stamen-derived bioactive gibberellin is essential for male flower development of Cucurbita maxima L. J Exp Bot 63: 2681–2691.
8. Ribeiro DM, Araujo WL, Fernie AR, Schippers JH, Mueller-Roeber B (2012) Translatome and metabolome effects triggered by gibberellins during rosette growth in Arabidopsis. J Exp Bot 63: 2769–2786.
9. Dayan J, Voronin N, Gong F, Sun TP, Hedden P, et al. (2012) Leaf-induced gibberellin signaling is essential for internode elongation, cambial activity, and fiber differentiation in tobacco stems. Plant Cell 24: 66–79.
10. Nadeau CD, Ozga JA, Kurepin LV, Jin A, Pharis RP, et al. (2011) Tissue-specific regulation of gibberellin biosynthesis in developing pea seeds. Plant Physiol 156: 897–912.
11. Hedden P, Phillips AL (2000) Gibberellin metabolism: new insights revealed by the genes. Trends Plant Sci 5: 523–530.
12. Spray CR, Kobayashi M, Suzuki Y, Phinney BO, Gaskin P, et al. (1996) The dwarf-1 (dt) Mutant of Zea mays blocks three steps in the gibberellin-biosynthetic pathway. Proc Natl Acad Sci U S A 93: 10515–10518.
13. Albone KS, Gaskin P, Macmillan J, Phinney BO, Willis CL (1990) Biosynthetic origin of gibberellins A(3) and A(7) in cell-free preparations from seeds of Marah macrocarpus and Malus domestica. Plant Physiol 94: 132–142.
14. Ko DH, Jun SH, Park HD, Song SH, Park KU, et al. (2010) Multiplex enzyme assay for galactosemia using ultraperformance liquid chromatography-tandem mass spectrometry. Clin Chem 56: 764–771.
15. Laverdiere I, Caron P, Couture F, Guillemette C, Levesque E (2012) Liquid chromatography-coupled tandem mass spectrometry based assay to evaluate inosine-5 ′-monophosphate dehydrogenase activity in peripheral blood mononuclear cells from stem cell transplant recipients. Anal Chem 84: 216–223.
16. Spacil Z, Elliott S, Reeber SL, Gelb MH, Scott CR, et al. (2011) Comparative triplex tandem mass spectrometry assays of lysosomal enzyme activities in dried blood spots using fast liquid chromatography: application to newborn screening of pompe, fabry, and hurler diseases. Anal Chem 83: 4822–4828.
17. Williams J, Phillips AL, Gaskin P, Hedden P (1998) Function and substrate specificity of the gibberellin 3beta-hydroxylase encoded by the Arabidopsis GA4 gene. Plant Physiol 117: 559–563.
18. Hu JH, Mitchum MG, Barnaby N, Ayele BT, Ogawa M, et al. (2008) Potential sites of bioactive gibberellin production during reproductive growth in Arabidopsis. Plant Cell 20: 320–336.
19. Martin DN, Proebsting WM, Hedden P (1997) Mendel's dwarfing gene: cDNAs from the Le alleles and function of the expressed proteins. Proc Natl Acad Sci U S A 94: 8907–8911.
20. Yamaguchi S, Smith MW, Brown RG, Kamiya Y, Sun T (1998) Phytochrome regulation and differential expression of gibberellin 3beta-hydroxylase genes in germinating Arabidopsis seeds. Plant Cell 10: 2115–2126.
21. Fukuda M, Matsuo S, Kikuchi K, Mitsuhashi W, Toyomasu T, et al. (2009) The endogenous level of GA1 is upregulated by high temperature during stem elongation in lettuce through LsGA3ox1 expression. J Plant Physiol 166: 2077–2084.
22. Hedden P, Phillips AL (2000) Gibberellin metabolism: new insights revealed by the genes. Trends Plant Sci 5: 523–530.
23. Lo SF, Yang SY, Chen KT, Hsing YI, Zeevaart JA, et al. (2008) A novel class of gibberellin 2-oxidases control semidwarfism, tillering, and root development in rice. Plant Cell 20: 2603–2618.
24. Mitchum MG, Yamaguchi S, Hanada A, Kuwahara A, Yoshioka Y, et al. (2006) Distinct and overlapping roles of two gibberellin 3-oxidases in Arabidopsis development. Plant J 45: 804–818.
25. Horimoto T, Koshioka M, Kubota S, Mander L, Hirai N, et al. (2011) Effect of warm and cold stratification on 1H-NMR profiles, endogenous gibberellins and abscisic acid in Styrax japonicus seeds. Hortic Environ Biotechnol 52: 233–239.
26. Xiao Y-H, Li D-M, Yin M-H, Li X-B, Zhang M, et al. (2010) Gibberellin 20-oxidase promotes initiation and elongation of cotton fibers by regulating gibberellin synthesis. J Plant Physiol 167: 829–837.
27. Arrua RD, Causon TJ, Hilder EF (2012) Recent developments and future possibilities for polymer monoliths in separation science. Analyst 137: 5179–5189.
28. Svec F (2012) Quest for organic polymer-based monolithic columns affording enhanced efficiency in high performance liquid chromatography separations of small molecules in isocratic mode. J Chromatogr A 1228: 250–262.
29. Svec F (2012) Porous polymer monoliths: amazingly wide variety of techniques enabling their preparation. J Chromatogr A 1217: 902–924.
30. Svec F, Frechet JMJ (1992) Continuous rods of macroporous polymer as high-performance liquid chromatography separation media. Anal Chem 64: 820–822.
31. Chen M-L, Fu X-M, Liu J-Q, Ye T-T, Hou S-Y, et al. (2012) Highly sensitive and quantitative profiling of acidic phytohormones using derivatization approach coupled with nano-LC–ESI-Q-TOF-MS analysis. J Chromatogr B 905: 67–74.
32. Brunauer S, Emmett PH, Teller E (1938) Adsorption of Gases in Multimolecular Layers. J Am Chem Soc 60: 309–319.
33. Barrett EP, Joyner LG, Halenda PP (1951) The Determination of Pore Volume and Area Distributions in Porous Substances. I. Computations from Nitrogen Isotherms. J Am Chem Soc 73: 373–380.
34. Stanelle RD, Sander LC, Marcus RK (2005) Hydrodynamic flow in capillary-channel fiber columns for liquid chromatography. J Chromatogr A 1100: 68–75.
35. Ma QA, Xu J, Lu Y, Shi ZG, Feng YQ (2010) Preparation of a mixed-mode of hydrophobic/cation-exchange polymer monolith and its application to analysis of six antidepressants in human plasma. Anal Methods 2: 1333–1340.
36. Brown JF, Krajnc P, Cameron NR (2005) PolyHIPE supports in batch and flow-through suzuki cross-coupling reactions. Ind Eng Chem Res 44: 8565–8572.
37. Frenette R, Friesen RW (1994) Biaryl synthesis via suzuki coupling on a solid support. Tetrahedron Lett 35: 9177–9180.
38. Lv YQ, Lin ZX, Svec F (2012) Hypercrosslinked large surface area porous polymer monoliths for hydrophilic interaction liquid chromatography of small molecules featuring zwitterionic functionalities attached to gold nanoparticles held in layered structure. Anal Chem 84: 8457–8460.
39. Chen ML, Liu YL, Xing XW, Zhou X, Feng YQ, et al. (2013) Preparation of a hyper-cross-linked polymer monolithic column and its application to the sensitive determination of genomic DNA methylation. Chem-Eur J 19: 1035–1041.
40. Urban J, Svec F, Frechet JMJ (2010) Efficient separation of small molecules using a large surface area hypercrosslinked monolithic polymer capillary column. Anal Chem 82: 1621–1623.
41. Chen M-L, Huang Y-Q, Liu J-Q, Yuan B-F, Feng Y-Q (2011) Highly sensitive profiling assay of acidic plant hormones using a novel mass probe by capillary electrophoresis-time of flight-mass spectrometry. J Chromatogr B 879: 938–944.
42. Chhun T, Aya K, Asano K, Yamamoto E, Morinaka Y, et al. (2007) Gibberellin regulates pollen viability and pollen tube growth in rice. Plant Cell 19: 3876–3888.
43. Liu S, Chen W, Qu L, Gai Y, Jiang X (2013) Simultaneous determination of 24 or more acidic and alkaline phytohormones in femtomole quantities of plant tissues by high-performance liquid chromatography-electrospray ionization-ion trap mass spectrometry. Anal Bioanal Chem 405: 1257–1266.